14th IMEKO TC10 Workshop on Technical Diagnostics
New Perspectives in Measurements, Tools and Techniques
for systems reliability, maintainability and safety
Milan, Italy, June 27-28, 2016

A probabilistic method to assess uncertainty in vision based modal analysis techniques

Alberto Lavatelli [1], Emanuele Zappa [2]

[1] Dept. of Mechanics, Politecnico di Milano, Via La Masa 1 20156 Milano, alberto.lavatelli@polimi.it
[2] Dept. of Mechanics, Politecnico di Milano, Via La Masa 1 20156 Milano, emanuele.zappa@polimi.it

***Abstract* - This paper addresses the problem of estimating uncertainty when recovering the basic modal parameters of a given mechanical system using a generic vision based displacement measurement system. The particular nature of photogrammetry makes the calculation of uncertainty a challenging task because of the complex phenomena that occur during image formation (motion blur, optical aberration, etc.). To overcome this problem, a Monte Carlo simulation of the whole measurement process (including structure dynamics and its impact on image formation) is proposed. In this way, it is possible to retrieve the posterior probability density functions (PDFs) for the identification of main modal parameters (resonant frequencies and amplitudes). Eventually the proposed probabilistic framework is a suitable tool to assess the performance of a vision based monitoring system on the design stage.**

Keywords: Uncertainty analysis; Vision based vibration monitoring; Monte Carlo method;

1. INTRODUCTION

In the relevant field of structural health monitoring (SHM) is possible to highlight several possible applications of vision based monitoring techniques. In particular, the possibility to measure the displacement of several monitored points without directly instrumenting those pushes the interest toward the application of image based vibration measurement system.

Even if vision based SHM systems have been proposed, the application of those techniques is still limited. One main reason is the difficulty found in the management of uncertainty. In fact, the process of image formation when dealing with moving targets, variable lighting and optical non-linearity is hardly predictable. In some circumstances (such as indoor tests of highly regular mechanical systems) it may be possible to describe the whole image formation process, so that all the parameters of optical transfer function are known. Nonetheless, the effect of motion blur, lighting variations and optical aberration on the final measurement accuracy is different with respect to each possible image analysis technique. Therefore, also the uncertainty connected to the extraction of metrological information from a set of images is hard to predict.

Furthermore, the dynamic behavior of actual structures is itself uncertain: given a certain input, the frequency response in terms of displacement and acceleration is variable by stochastic means [1][2][3][4][5]. Given those premises, the aim of this paper is to find a robust solution to approach the problem of uncertainty estimation when monitoring a vibrating mechanical system with vision based measurement system.

2. MONTE CARLO SIMULATION

The approach proposed by the authors sees the application of Monte Carlo methodology in order to simulate the whole measurement process. This choice is claimed to be the most accurate when estimating uncertainty of complex measurement systems [6][7][8]. Firstly, an image based measurement technique to evaluate is selected. Then it is necessary to select a structure to be monitored and recover a dynamic response model as a set of Laplace domain transfer functions (LTI model). The variability of structural response is represented by sampling modal parameters (mainly natural frequencies and damping ratios) from suitable probability density functions (PDFs).

Then it is necessary to sample a structural excitation time history $F(t)$, by means of parametric analytic functions $F_0(t, p_1, p_2, , p_n)$ having the p_n parameters of eq.(1) sampled from appropriate PDFs. It is also possible to add some process noise $N_p(t)$.

$$F(t) = F_0(t, p_1, p_2, , p_n) + N_p(t) \tag{1}$$

The next step sees the simulation of mechanical response by inputting structural excitation into the LTI model. Consequently, an ideal displacement time history $x_{ID}(t)$ is retrieved. Then, by using a displacement transducer model, it is possible to calculate the measured displacement $x_{TR}(t)$ from $x_{ID}(t)$. At the same time the ideal displacement time history is used to simulate the image formation process. In particular, it is possible to take into account motion blur, optical aberration and lighting changes using a proper image formation model that will be further discussed. Once the images of vibrating target are recovered, it is possible to send them to the processing stage, where the vision based method is used to recover a vision based displacement signal $x_{VIS}(t)$. Furthermore, starting from $F(t)$, the excitation measurement $\tilde{F}(t)$ is calculated from an appropriate transducer model.

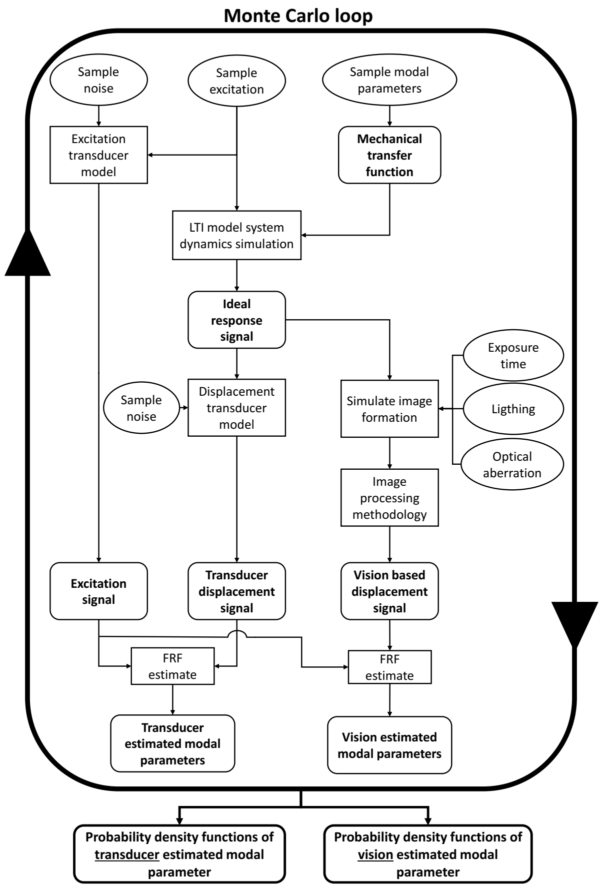

Fig. 1. Monte Carlo loop description: single realization of the monitored structure

Up to this stage of the algorithm, two displacement signals of structure are available: one coming from usual transducers $x_{TR}(t)$, another from vision system $x_{VIS}(t)$ and the excitation signal $\tilde{F}(t)$. Therefore, it is possible to send them to a transfer function estimation algorithm in order to estimate the modal parameters of interest. The previous sequence of operations provides a single realization of the value of monitored modal parameters for a given structure in case of traditional transducers and vision based measurement systems. By running those operations sequentially for a high number of times, we get the Monte Carlo loop described in Fig. 1.

A. Simulating image formation

The process of image formation is quite complex and it should be simulated by providing some simplifying assumptions. In particular, the rigid motion of the structure is simulated by phase shifting the Fourier Transform of the image of the target in equilibrium position [9]. Simultaneously motion blur is generated using the averaging algorithm [10]. This transformation is known as the EPSA (Exact Phase Shift and Averaging) algorithm. Then it is possible to add contrast stretch or amplification with operations on image histogram. Optical aberration may be modelled by resampling image with a quadratic or cubic radial aberration model. Other contributes (optical blur, noise..) can be modeled with appropriate image filters.

3. CASE STUDY: ANALYZING THE EFFECTS OF MOTION BLUR ON FRF ESTIMATION

A simple case study is proposed in order to evaluate the effects of motion blur on FRF estimation and validate the probabilistic architecture here proposed [11]. For the purpose of this paper, a linear time independent (LTI) model of the flexural behavior of a stadium grandstand is simulated. The parameters were extracted from [2]. The model represents the vertical displacement response of platform tip for a vertical force for the first three natural frequencies. It can be expressed as a parallel of three mono-modal transfer functions in the Laplace domain $G_i(s)$ in equation (2).

$$\begin{cases} G_i(s) = \frac{1}{\tilde{m}_i s^2 + 2\tilde{m}_i h_i \omega_i s + \tilde{m}_i \omega_i^2} \\ \omega_i = 2\pi \cdot f_i \end{cases} \quad (2)$$

Modal masses $\tilde{m}_i$ are fixed, while the natural frequencies f_i and damping ratios h_i are random variables. The stochastic nature of f_i is represented by normal PDFs, while the variability of damping ratios is expressed by a random uniform variable. The PDFs for each variable are listed in Table 1. The assumptions on probability distributions of modal parameters comes from the analysis of a set of data of the authors' personal experience as well as from a review of documented experimental cases found in scientific literature [12][13].

Table 1. PDFs of structural response variability

Variable	PDF	Mean value	Std. dev
f_1	Normal	2.0	0.1
h_1	Uniform	0.06	0.0014
f_2	Normal	2.5	0.05
h_2	Uniform	0.03	0.0003
f_3	Normal	3.16	0.2
h_3	Uniform	0.15	0.0029

The modal testing system simulated in this paper is a simple decay test. The excitation force is transduced by a simulated load cell having a signal-to-noise ratio (SNR) equal to 5. The displacement $x_{TR}(t)$ is transduced by a simulated TOF laser having SNR equal to 10. In this case the authors considered to simulate correctly calibrated instruments, for which the transducers noise can be modeled as zero-mean Gaussian. Structure excitation is modeled with equation 3, where α is a random uniform variable with mean 5.6 and standard deviation 0.0115. Excitation peak F_0 is $1000 \pm 50\,\mathrm{N}$ uniformly distributed. Process noise $N_p(t)$ is zero mean Gaussian with standard deviation equal to $100\,\mathrm{N}$.

$$F(t-t_0) = \frac{F_0}{e \cdot \alpha} \cdot te^{-\alpha(t-t_0)} + N_p(t) \tag{3}$$

For the purpose of this paper, all contributes to uncertainty related to instrument calibration are neglected. Both the signals are sampled at $50\,\mathrm{Hz}$ and processed using the well-known Welch periodogram method in order to estimate the structural FRF. The estimated FRF is calculated with a frequency resolution of $0.01\,\mathrm{Hz}$. In order to avoid windowing problems, the excitation starts at t_0 =33 s.

In this case study, the modal parameters monitored are the first two resonant frequencies f_1, f_2 and their relative resonant amplitudes a_1, a_2 (which are the amplitude of estimated FRF at the estimated resonant frequencies). Resonant frequencies are identified by peak picking the absolute value of the imaginary part of FRF. Since the structures displacement is monitored at the same time by a classic transducer and by a vision technique, it is possible to compare the estimation of the fore mentioned modal provided by the vision system with the reference one provided by TOF laser.

A. *Imaging technique and investigation path*

For what concerns the case study here presented, vibrations are monitored with a simple 2D blob detection method. The simulated blob consists in a bright circle on a black background. The luminance profile of the blob is flat with edges smoothed by a Gaussian blur. Blob detection is carried out by a fixed threshold, then the centroid of the bright region is computed.

For each sample of structure displacement, the reference blob image is proportionally translated. For the purpose of this paper, the amount of translation is directly proportional to $x_{ID}(t)$ by means of a simple scaling factor equal to $20\,\mathrm{px/mm}$. Up to now, an image of the tracked blob without motion blur is available for each sample of the actual displacement of structure $x_{ID}(t)$ (in fact the frames are virtually shot with infinitesimal exposure time as in Fig.2a).

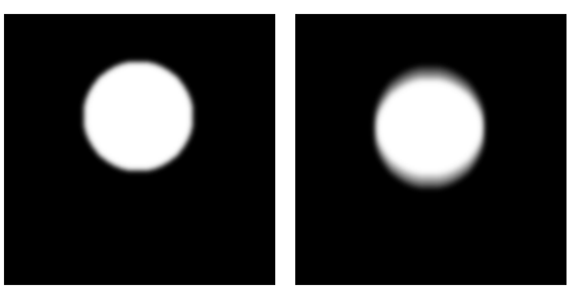

(a) (b)

Fig. 2. Tracked blob at peak of excitation. On the left the ideal image of marker, on the right motion blur simulation (exposure time $140\,\mathrm{ms}$)

As said previously, the aim of this work is to investigate the effect of motion blur. This is done by averaging the rigidly translated blob images up to a specified exposure time [10]. In this way the actual physics of motion blur formation is simulated: during exposure time the blob travels through the recorded scene. The final result of this procedure is shown in Fig.2b where it is possible to see how motion blur smeares shapes by convuluting marker motion with the acquisition window.

In this case study nine levels of exposure times are tested: 40, 60, 80, 100, 120, 140, 160 and $180\,\mathrm{ms}$. The specified path corresponds to exposure to period ratios $E2PR$ [14] spanning from 0.04 up to 0.4. The testing path here described investigates motion blur starting from the typical condition of a performing experimental setup (where $E2PR$ spans in the range 0.01-0.08 [14]) ending to high motion blur situations (where exposure is about 40% of the vibration period). Higher exposure configurations have not been tested due to the obvious impossibility to measure due to aliasing.

B. *Monte Carlo loop and probabilistic analysis*

For each value of exposure time, the Monte Carlo analysis saw the realization of 1000 structure excitation and modal parameter estimation. Each realization saw the simulation of $100\,\mathrm{s}$ of system dynamics, for a total amount of 27 h 46 min and 40 s of simulated response for each value of exposure time.

At the end of simulation, for each value of frequency it was possible to retrieve 1000 realizations of FRF for both vision and transducer, consequently 1000 realizations of modal parameters. From this set of values it was possible to compute the posterior PDFs and their relative cumulative density functions (CDFs). Then it was possible to estimate, for each frequency value, the mean value of FRF and 90% confidence bounds from the posterior CDFs.

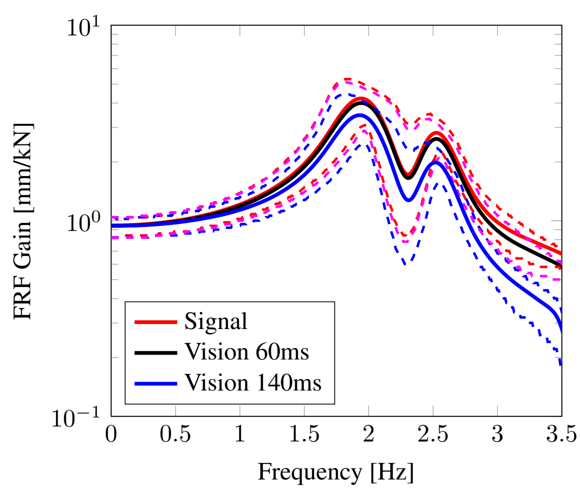

Fig. 3. FRF gain diagram for both monitoring techniques with 90% confidence bounds (exposure time $140\,\mathrm{ms}$ and $60\,\mathrm{ms}$).

To sum up, as a final output, for each value of exposure time tested in this case study and for both vision and transducer, it was possible to retrieve: estimated FRF with mean and posterior confidence bounds, PDFs of estimated resonant frequencies and PDFs of estimated resonant amplitudes. Eventually, uncertainty is not treated by postulating a particular uncertainty model, but it is computed as is from the simulation data.

C. Discussion of simulation results: motion blur as a particular kind of filter

Once the system has been simulated for all the values of exposure time, it is possible to analyze data of FRF estimation and modal parameters in order to draw some conclusions. In Fig.3 it is possible to see the overall effects on FRF estimation. The vision-estimated response appears smaller in magnitude and more damped in average. The confidence bounds are similar in shape with respect to the transducer-based estimation. By looking at the diagrams of Fig.4, it is possible to state that using a vision system instead of a transducer has no effect on the identification of natural frequencies, since both the measurement system are able displays identical identification statistics. Or, at least, no effect is recognizable until exposure time is lower than the frequency aliasing threshold.

Conversely, the process of resonant amplitude identification is affected by the use of vision techniques. The statistical analysis highlights that the presence of a finite exposure time leads to an underestimation of a_1, a_2. As a general trend, the higher the exposure time, the lower is the identified resonant amplitude.

In Fig.5, the statistics of resonant amplitude identification process are plotted for each value of exposure time. As a result, a graph displaying the standard deviation of identified amplitude σ_A as a function the mean value of identified amplitude μ_A is shown. As exposure time and motion blur increase, not only the mean value of resonant amplitude decreases, but also the standard deviation of resonant amplitudes decreases . This result is itself interesting:

- as a first effect, motion blur acts as a mobile average filter. This is an expected phenomenon and it explains why the mean value of resonant amplitude is shifted to lower value with respect to a classic transducer. As any mobile average filter [15] it decreases the useful bandwidth of transfer function estimation with a sinc kernel. In particular motion blur produces a clipping of the vibration amplitude at the peak of the sinusoidal motion, as demonstrated in [10].

- A second effect of motion blur is to decrease the standard deviation of resonant amplitude estimation. This phenomenon might lead to the incorrect and risky conclusion that the uncertainty on amplitude estimation is reduced. A physical interpretation of this phenomenon is not found in literature. However in authors' opinion, the phenomenon of clipping at the inversion point restrains the space of observable states of the system. In other words, as motion blur increases, it is possible to have a set of system configurations that can produce the same measured transfer function due to the filtering effect of the convolution phenomenon.

To sum up, using vision based measurement techniques to monitor vibrations may produce a relevant bias in the evaluation of physical properties of mechanical systems. In the case here discussed, the apparent stiffness is lower and less variable with respect to the ideal case. This phenomenon is triggered by motion blur: the higher is $E2PR$, the lower the estimated resonant amplitude. For the system discussed in this case study, the $E2PR$ limit for accurate FRF estimation is about 0.12. Higher values of exposure will produce estimation errors higher than 10% of the nominal values.

In Fig.6 the width of FRF uncertainty band is plotted as a function of frequency. In this case the presence of a fictitious decrease of uncertainty is detectable in all the process of FRF estimation. As a consequence the estimation of modal parameters in a single run appears more reliable. This behavior is potentially dangerous in the field of model based SHM, where the value of SNR and the stability of modal parameters are often used to judge the accordance of the experimental behavior of a structure with the one predicted by a model.

D. Evaluating the uncertainty contribute of the measurement method

One last analysis available within the proposed uncertainty estimation framework is the evaluation of the uncertainty generated by the modal analysis method. This is done by erasing the uncertainties of structural response so that the standard deviation of the parameters listed in Table 1 is identically equal to 0.

In this way, an ideal noise-free transducer should provide a perfect identification of modal parameters, which should be estimated without uncertainty. Conversely all transducer models used in the Monte Carlo simulation take into account disturbs such as electrical noise for analog sensors and motion blur for cameras. Nonetheless, structural excitation model takes into account process noise. As a consequence the measurement method itself introduces uncertainty in the estimation of modal parameters, even in the case of an ideal structure [2]. To sum up, it is possible to provide estimation of measurement uncertainty for the generic modal parameter.

In Table 2 the results of modal parameter estimation at various levels of exposure are listed. Table 2 reports for the first two modes the following quantities: the value of exposure time t_{sh}, the mean value of resonant amplitude μ_A, the standard deviation of resonant amplitude σ_A, the mean value of resonant frequency μ_F and the standard deviation of resonant frequency σ_F. For what concerns the method used in this case study, the results confirms that motion blur is able to alter the output of modal analysis by introducing measurement bias and changing the apparent

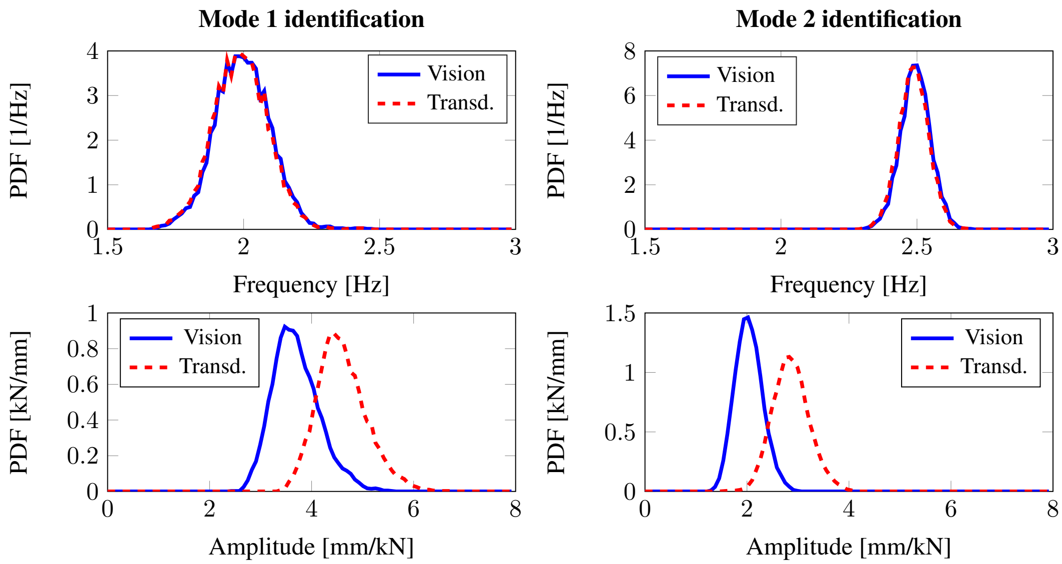

Fig. 4. Posterior PDFs of modal parameters identification for exposure time equal to 140ms.

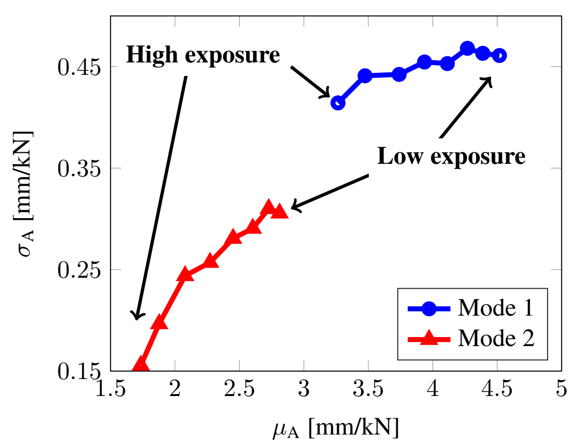

Fig. 5. Statistics of identification of resonant amplitudes for the vision based system as motion blur increases

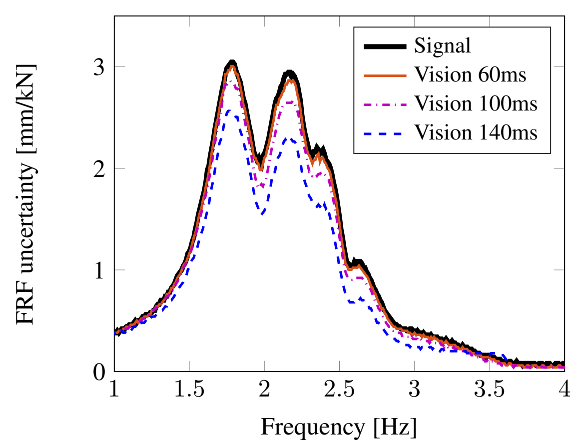

Fig. 6. Uncertainty of FRF amplitude estimation (with 90% level of confidence) for different values of exposure time

measurement uncertainty on FRF amplitude estimation. A further representation of this phenomenon can be found in Fig.7 where the plot of σ_A as a function of μ_A is displayed.

For what concerns the estimation of natural frequencies, it is possible to state that the vision based methodology here discussed is not sensitive to motion blur. In fact for both the modes, μ_F and σ_F are almost constant in value as exposure changes. Conversely it is possible to see a clear trend for μ_A and σ_A, since both monotonically decrease in value as motion blur increases. At low level of exposure the decreasing slope is quite slow, conversely at high level of exposure the decreasing slope is steep, resulting in a non linear behavior.

The results also confirm the disguising behavior of motion blur. In fact the presence of this contribute at low $E2PR$ values is indeed negligible for a good estimation of modal parameters. However the $E2PR$ depends not only on the exposure time, but also on the period of vibration. Hence each natural frequency is characterized by a different value of $E2PR$. In conclusion, the estimation of uncertainty in this context is not only related to the method itself, but also on the dynamics of the oscillating system under analysis.

4. CONCLUSION

In this paper the authors proposed a probabilistic method to evaluate the uncertainty of mechanical transfer

Table 2. Uncertainty of the vision based modal parameter estimation method for a set of exposure time values

	Mode 1				Mode 2			
[ms]	[mm kN^{-1}]		[Hz]		[mm kN^{-1}]		[Hz]	
t_{sh}	μ_A	σ_A	μ_F	σ_F	μ_A	σ_A	μ_F	σ_F
40	4.44	0.32	2.01	0.01	2.78	0.24	2.50	0.01
60	4.36	0.31	2.01	0.01	2.69	0.22	2.50	0.01
80	4.23	0.31	2.00	0.01	2.57	0.21	2.50	0.01
100	4.07	0.28	2.01	0.01	2.42	0.20	2.51	0.01
120	3.90	0.27	2.00	0.01	2.25	0.18	2.50	0.01
140	3.67	0.25	2.01	0.01	2.05	0.16	2.50	0.01
160	3.45	0.24	2.01	0.01	1.83	0.14	2.51	0.01
180	3.21	0.22	2.00	0.01	1.67	0.10	2.50	0.01

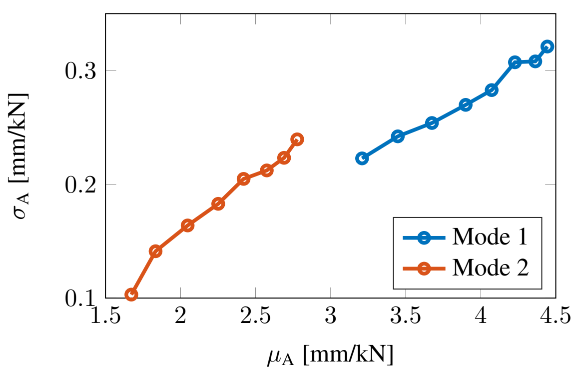

Fig. 7. Trends of apparent uncertainty reduction due to motion blur for the vision method analyzed

estimation when a generic vision based method is used to sense mechanical vibrations.

The method exploits the well-known Monte Carlo framework to simulate the behavior of a mechanical systems. The knowledge of optical phenomena let the experimenter model all the process of image formation, in order to weight correctly the capabilities of a generic vision based measurement technique.

In order to show the possible use of the proposed method, a simple case study is discussed, where the effects of motion blur in a simple blob detection method are analyzed. In particular the attention is focused on the uncertainty and on the bias of amplitude FRF estimation due to the effect of motion blur. As a final result it was possible to estimate the maximum amount of $E2PR$ (the ratio between exposure time and displacement period) that allows accurate measurement of modal parameters.

REFERENCES

[1] S. Adhikari, M. Friswell, K. Lonkar, and A. Sarkar, "Experimental case studies for uncertainty quantification in structural dynamics," *Probabilistic Engineering Mechanics*, vol. 24, no. 4, pp. 473 – 492, 2009.

[2] A. Cattaneo, S. Manzoni, and M. Vanali, "Measurement uncertainty in operational modal analysis of a civil structure," in *Proceedings of ISMA 2010 - International Conference on Noise and Vibration Engineering, including USD 2010*, pp. 5103–5115, 2010.

[3] M. Shinozuka, "Structural response variability," *Journal of Engineering Mechanics*, vol. 113, no. 6, pp. 825–842, 1987.

[4] C. Bucher and M. Shinozuka, "Structural response variability ii," *Journal of Engineering Mechanics*, vol. 114, no. 12, pp. 2035–2054, 1989.

[5] A. Kardara, C. Bucher, and M. Shinozuka, "Structural response variability iii," *Journal of Engineering Mechanics*, vol. 115, no. 8, pp. 1726–1747, 1989.

[6] R. Mullen and R. Muhanna, "Probability bounds for the system response of non-linear structures," in *Safety, Reliability, Risk and Life-Cycle Performance of Structures and Infrastructures - Proceedings of the 11th International Conference on Structural Safety and Reliability, ICOSSAR 2013*, pp. 499–502, 2013.

[7] M. Damgaard, L. Andersen, L. Ibsen, H. Toft, and J. Srensen, "A probabilistic analysis of the dynamic response of monopile foundations: Soil variability and its consequences," *Probabilistic Engineering Mechanics*, vol. 41, pp. 46–59, 2015.

[8] S. Mukhopadhyay, R. Betti, and H. Lus, "Structural identification and uncertainty quantification in operational modal analysis with minimal instrumentation," in *Safety, Reliability, Risk and Life-Cycle Performance of Structures and Infrastructures - Proceedings of the 11th International Conference on Structural Safety and Reliability, ICOSSAR 2013*, pp. 1879–1884, 2013.

[9] P. Reu, "Experimental and numerical methods for exact subpixel shifting," *Experimental Mechanics*, vol. 51, no. 4, pp. 443–452, 2011.

[10] E. Zappa, A. Matinmanesh, and P. Mazzoleni, "Evaluation and improvement of digital image correlation uncertainty in dynamic conditions," *Optics and Lasers in Engineering*, vol. 59, pp. 82–92, 2014.

[11] Q. Huang, P. Gardoni, and S. Hurlebaus, "Assessment of modal parameters considering measurement and modeling errors," *Smart Structures and Systems*, vol. 15, no. 3, pp. 717–733, 2015.

[12] I. Behmanesh and B. Moaveni, "Accounting for environmental variability, modeling errors, and parameter estimation uncertainties in structural identification," *Journal of Sound and Vibration*, vol. 374, pp. 92 – 110, 2016.

[13] E. Reynders, K. Maes, G. Lombaert, and G. D. Roeck, "Uncertainty quantification in operational modal analysis with stochastic subspace identification: Validation and applications," *Mechanical Systems and Signal Processing*, vol. 6667, pp. 13 – 30, 2016.

[14] G. Busca, G. Ghislanzoni, and E. Zappa, "Indexes for performance evaluation of cameras applied to dynamic measurements," *Measurement: Journal of the International Measurement Confederation*, vol. 51, no. 1, pp. 182–196, 2014.

[15] G. D'Antona and A. Ferrero, *Digital Signal Processing for Measurement Systems: Theory and Applications*. Information Technology: Transmission, Processing and Storage, Springer US, 2006.